Journal of Pharmacological Sciences 133 (2017) 70–78

Contents lists available at ScienceDirect

Journal of Pharmacological Sciences

journal homepage: www.elsevier.com/locate/jphs

Full paper

Machine learning-based prediction of adverse drug effects: An example of seizure-inducing compounds

Mengxuan Gao [a, b], Hideyoshi Igata [a], Aoi Takeuchi [a], Kaoru Sato [b, c], Yuji Ikegaya [a, b, d, *]

[a] Graduate School of Pharmaceutical Sciences, The University of Tokyo, Tokyo 113-0033, Japan
[b] iPS-non Clinical Experiments for Nervous System (iNCENS) Project, Japan
[c] Division of Pharmacology, National Institute of Health Sciences, Tokyo 158-8501, Japan
[d] Center for Information and Neural Networks, National Institute of Information and Communications Technology, Osaka 565-0871, Japan

ARTICLE INFO

Article history:
Received 28 September 2016
Received in revised form
8 January 2017
Accepted 13 January 2017
Available online 28 January 2017

Keywords:
Artificial intelligence
Side effect
Epilepsy
Clinical
Toxicity

ABSTRACT

Various biological factors have been implicated in convulsive seizures, involving side effects of drugs. For the preclinical safety assessment of drug development, it is difficult to predict seizure-inducing side effects. Here, we introduced a machine learning-based *in vitro* system designed to detect seizure-inducing side effects. We recorded local field potentials from the CA1 alveus in acute mouse neocortico-hippocampal slices, while 14 drugs were bath-perfused at 5 different concentrations each. For each experimental condition, we collected seizure-like neuronal activity and merged their waveforms as one graphic image, which was further converted into a feature vector using Caffe, an open framework for deep learning. In the space of the first two principal components, the support vector machine completely separated the vectors (*i.e.*, doses of individual drugs) that induced seizure-like events and identified diphenhydramine, enoxacin, strychnine and theophylline as "seizure-inducing" drugs, which indeed were reported to induce seizures in clinical situations. Thus, this artificial intelligence-based classification may provide a new platform to detect the seizure-inducing side effects of preclinical drugs.

1. Introduction

Convulsive seizures involve body shakes that occur rapidly and uncontrollably and are often associated with a loss of consciousness. Seizures generally result from the excessive excitation and synchronization of neurons. Factors that cause hyperactive and synchronous states of neuronal networks involve i) remodeling of synaptic connections (1), ii) changes in extracellular ion concentrations (2), iii) the modification of neurotransmitters and their receptors (3, 4), and iv) medications, *i.e.*, adverse effects (AEs) of drugs (5, 6). In the central nervous system, seizures are one of most severe AEs, leading to a decline in development or withdrawal from the market. In the preclinical safety assessment of drug development, animal experiments are used to screen drugs that potentially exhibit such AEs; however, it is difficult to detect drugs that exert seizure-inducing effects.

Hippocampal slices can be used for *in vitro* epilepsy models and pharmacological validation (7). Epileptiform hyperactivity is induced by proconvulsants (8), electrical stimulation (9), and extracellular ionic changes (10). In these cases, seizure-like events (SLE), as sustained synchronous neuronal discharges, are considered hallmarks (2) and are detectable in local field potentials (LFPs). However, human bias-free and clear-cut criteria to predict the onset of seizure are also required in the analysis of *in vitro* data. The new assessment system based on the recording of LFPs from hippocampal slices may provide a method to identify the seizure-inducing effects of drugs.

In the present study, we treated brain slices, including the hippocampus, with a total of 14 drugs that either do or do not induce seizures in humans. By recording LFPs from the alveus, we automatically detected SLEs in LFP traces using an image recognition technique. Specifically, we used the deep learning network Caffe to extract the features from LFP images and identified SLEs using a linear support vector machine (SVM) in the state space whose dimension was reduced using principal component analysis

* Corresponding author. Laboratory of Chemical Pharmacology, Graduate School of Pharmaceutical Sciences, The University of Tokyo, 7-3-1 Hongo, Bunkyo-ku, Tokyo 113-0033, Japan. Fax: +81 3 5841 4786.
E-mail address: yuji@ikegaya.jp (Y. Ikegaya).
Peer review under responsibility of Japanese Pharmacological Society.

http://dx.doi.org/10.1016/j.jphs.2017.01.003

(PCA). The correct rate of prediction obtained using the cross-validation test was 100%. All drugs used here were perfectly assigned as either safe or seizure-inducing drugs.

2. Materials and methods

2.1. Animals

The animal experiments were performed with the approval of the Animal Experiment Ethics Committee at the University of Tokyo (approval number: P24-8) and according to the University of Tokyo guidelines for the Care and Use of Laboratory Animals. Male ICR mice (3- to 4-week-old) were housed under standard laboratory conditions (12-h light/12-h dark cycle, free access to food and water). These experimental protocols were conducted in accordance with the Fundamental Guidelines for Proper Conduct of Animal Experiment and Related Activities in Academic Research Institutions (Ministry of Education, Culture, Sports, Science and Technology, Notice No. 71 of 2006), the Standards for Breeding and Housing of and Pain Alleviation for Experimental Animals (Ministry of the Environment, Notice No. 88 of 2006), and the Guidelines on the Method of Animal Disposal (Prime Minister's Office, Notice No. 40 of 1995).

2.2. Drugs

Aspirin, cimetidine, dextran, diazepam, diphenhydramine, enoxacin, ibuprofen, imipramine, isoniazid, ketamine, methamphetamine, metoclopramide, oseltamivir, picrotoxin, strychnine, and theophylline were used. Aspirin and theophylline were dissolved at a stock concentration of 50 mM in 33% dimethyl sulfoxide (DMSO), and the final concentrations of these drugs were adjusted to contain 2% DMSO. Dextran was dissolved at a stock concentration of 10% w/v immediately prior to use. Diazepam was dissolved at a stock concentration of 1 mM in a solution comprising 40% propylene glycol and 10% ethanol in double-distilled water. Ibuprofen was dissolved at a stock concentration of 25 mM in 50% DMSO, and its final concentration contained less than 0.6% DMSO. The other drugs were dissolved in double-distilled water at various stock concentrations, stored at 4 °C, and diluted 1:100–100,000 (Table 1) immediately prior to use in artificial cerebrospinal fluid (aCSF) with a low extracellular magnesium ion concentration ($[Mg^{2+}]_e$), comprising (in mM) 127 NaCl, 3.5 KCl, 1.24 KH_2PO_4, 0.1 $MgSO_4$, 2.0 $CaCl_2$, 26 $NaHCO_3$ and 10 D-glucose.

2.3. Slice preparations

Acute slices were prepared from the ventral part of the hippocampal formation in 3- to 4-week-old ICR male mice (SLC, Shizuoka, Japan). The mice were anesthetized with isoflurane, followed by decapitation, and the brain was horizontally sliced at a thickness of 400 μm in the fronto-occipital direction using a vibratome in ice-cold oxygenated modified aCSF comprising (in mM) 222.1 sucrose, 27 $NaHCO_3$, 1.4 NaH_2PO_4, 2.5 KCl, 0.5 ascorbic acid, 1 $CaCl_2$, and 7 $MgSO_4$. Subsequently, the slices were maintained in normal ACSF comprising (in mM) 127 NaCl, 3.5 KCl, 1.24 KH_2PO_4, 1.2 $MgSO_4$, 2.0 $CaCl_2$, 26 $NaHCO_3$, and 10 D-glucose and bubbled with 95% O_2 and 5% CO_2 at 37 °C for at least 1 h. One to three slices per mouse were used in the following experiments.

2.4. Local field potential recording

A brain slice, which included the hippocampus and the temporal neocortex, was placed on an 8 × 8 planar multi-electrode array (MED-P515A, Alpha MED Scientific; electrode size: 50 × 50 μm; inter-polar interval: 150 μm) and maintained in the interface condition at 35 °C. Low $[Mg^{2+}]_e$ aCSF was bubbled with 95% O_2 and 5% CO_2 at room temperature. aCSF was perfusion at a flow rate of 1 ml/min using a peristaltic pump. As the bath volume of the chamber was 0.8 ml, aCSF was thought to be replaced with new aCSF within about 1 min. Based on the total volume of the inlet tube, the onset time at which the solution reached the chamber was defined as the time at which the solution was switched. LFPs were simultaneously acquired from the 64 recording electrodes of the multi-electrode arrays and digitalized at 10 kHz using an Alpha MED Scientific system.

2.5. Data analysis

The data were exported at 1 kHz and processed using custom-made routines in Matlab (The MathWorks, Natick, MA, USA). The raw data were hamming-filtered with a time window of 30 ms (11) and differentiated at an interval of 50 ms. The peaks were automatically detected when their absolute values exceeded 0.1 μV/ms. To ensure that the drug concentration in the chamber reached to objective values during the occurrence of the peaks, for each 10-min trace of a certain concentration, the first and last 1 min were cut out from analysis. For each peak, the LFP trace form −200 to 2070 ms relative to the peak was transformed into a 227 × 227-pixel binary picture, and the horizontal and vertical axis showed

Table 1
Concentrations of the drugs tested. Each drug was bath-applied at increasing concentrations as shown in the table. The values in the gray-shaded cells represent the clinical blood concentrations of the corresponding drugs in healthy persons.

	Stock concentration	Bath concentrations					
Aspirin	50 mM	30	100	300	1000	3000	μM
Cimetidine	10 mM	1	3	10	30	100	μM
Dextran	10 w/v %	0.003	0.01	0.03	0.1	0.3	w/v %
Diazepam	1 mM	0.1	0.3	1	3	10	μM
Diphenhydramine	50 mM	1	3	10	30	100	μM
Enoxacin	25 mM	1	3	10	30	100	μM
Ibuprofen	25 mM	3	10	30	100	300	μM
Imipramine	10 mM	0.1	0.3	1	3	10	μM
Isoniazid	100 mM	10	30	100	300	1000	μM
Ketamine	50 mM	1	3	10	30	100	μM
Methamphetamine	50 mM	1	3	10	30	100	μM
Metoclopramide	10 mM	0.1	0.3	1	3	10	μM
Oseltamivir	10 mM	1	3	10	30	100	μM
Picrotoxin	5 mM	1	3	10	30	100	μM
Strychnine	25 mM	0.3	1	3	10	30	μM
Theophylline	50 mM	30	100	300	1000	3000	μM

time at a resolution of 0.01 s/pixel and the mean voltage at resolution of 1 μV/pixel (between −50 μV and 177 μV), respectively; that is, the mean voltage was calculated every 10 ms. For each concentration of a drug, the binary image of all the LFP peaks was superimposed into a single 227 × 227 binary picture file.

2.6. Machine learning-based classification

The pictures were converted to feature vectors using the BVLC CaffeNet Model in the Caffe library (Berkeley Vision and Learning Center, USA). Caffe provides a deep convolutional neural network pre-trained using datasets in Large Scale Visual Recognition Challenge 2012 (12). The sixth layer of Caffe, called fc6, where each image was represented in a 4096-dimensional vector, was used as the input features in PCA-based SVM. First, the vectors were re-coordinated using PCA (13), and the feature datasets in the first two principal components (PC1 and PC2) were separated using linear SVM (14). Leave-one-out cross-validation was used to verify the data separation, and the F1 score, sensitivity, and specificity were calculated to evaluate the accuracy of the prediction (15).

3. Results

3.1. Low $[Mg^{2+}]_e$ conditions induce synchronous LFP activity

Low $[Mg^{2+}]_e$ conditions enhance neuronal network excitability and increase the incidence of synchronous epileptiform activity in rodent hippocampal slices (2, 10). We thus reasoned that reducing $[Mg^{2+}]_e$ enhances the power to detect the SLE-inducing effect of drugs. When recording LFPs in acute cortico-hippocampal slices using a 64-channel electrode array (Fig. 1A), the $[Mg^{2+}]_e$ was reduced from 1.2 to 0.1 mM. In normal $[Mg^{2+}]_e$ aCSF (1.2 mM), neuronal activity was not evident in LFPs; however, when low $[Mg^{2+}]_e$ aCSF (0.1 mM) was bath-perfused, spontaneous LFP activity repetitively emerged (Fig. 1B). The LFP activity was simultaneously recorded from multiple electrode channels, indicating that these events were synchronized at the network level (Fig. 1C). The activity was diverse in spatiotemporal patterns, likely originating from either the neocortex or the hippocampus based on the time lags of the event onsets and the LFP amplitudes of the events (data not shown). Thus, the activity events were reliably detected in LFP traces recorded from the alveus, the border area (white matter) between the neocortex and the hippocampus (*e.g.*, the red circle in Fig. 1A). In the following sections, we employed 0.1 mM $[Mg^{2+}]_e$ and analyzed LFP traces recorded from an electrode located on the alveus.

3.2. Picrotoxin induces SLEs

γ-Aminobutyric acid (GABA) is a major inhibitory neurotransmitter in the central nervous system, and its reduction causes epileptiform activity (16). We first examined the effects of picrotoxin, a $GABA_A$ receptor antagonist. Picrotoxin was bath-perfused at increasing concentrations of 0, 1, 3, 10, 30, and 100 μM for 10 min each. At concentrations higher than 10 μM, picrotoxin induced repetitive LFP activity with peak amplitudes larger than 30 μV (Fig. 2). Each LFP event comprised an initial large burst and a few cycles of small oscillations (Fig. 2 inset), a typical sign of the early phases of SLEs (17, 18).

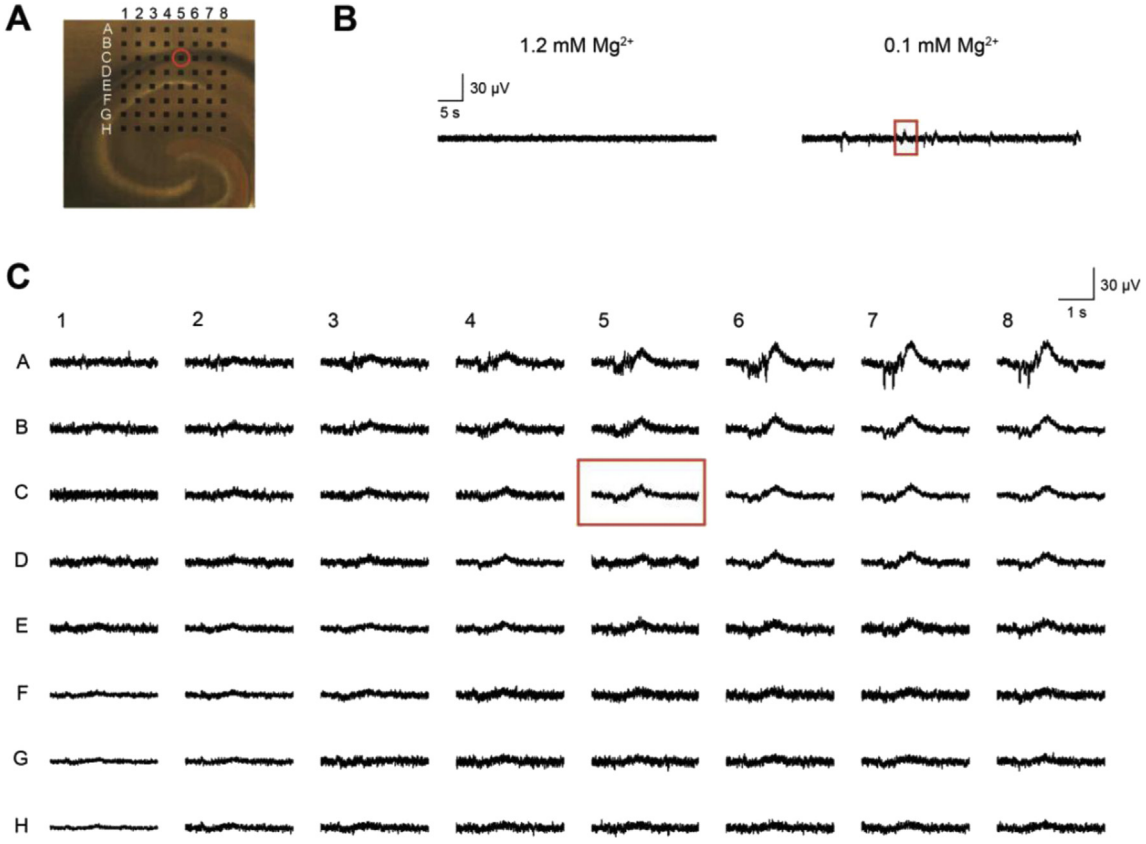

Fig. 1. LFP recordings using a 64-channel MEA. A: Arrangement of the 64 electrodes on an acute mouse hippocampal slice. B: Representative LFP traces recorded from an electrode on the hippocampal alveus (the C5 channel indicated as a red circle in (A)) were perfused with normal aCSF (left; 1.2 mM $[Mg^{2+}]_e$) and subsequently perfused with modified aCSF (right; 0.1 mM $[Mg^{2+}]_e$). Note that low $[Mg^{2+}]_e$ conditions induce spontaneous LFP activity. C: All 64 traces of the LFP event, boxed in (B), are expanded in the time axis, indicating that the event was synchronous across electrodes and might originate in the neocortex. The labels along the rows and the columns correspond to (A).

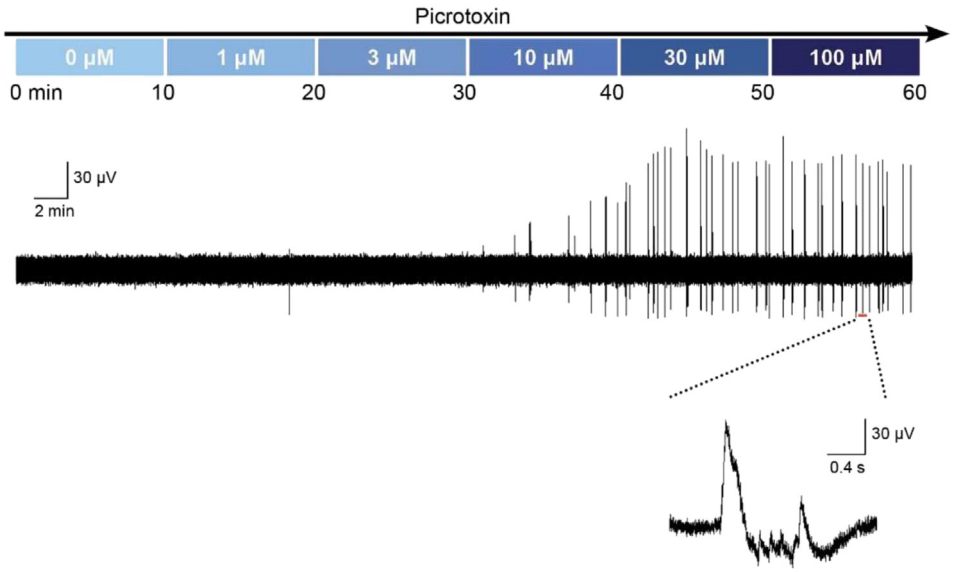

Fig. 2. Picrotoxin induces SLEs in a concentration-dependent manner. Representative LFP traces recorded from the alveus in a series of bath concentrations of picrotoxin ranging from 0 to 100 μM (indicated in the top bar). Picrotoxin was applied for 10 min at each concentration under 0.1 mM $[Mg^{2+}]_e$ conditions. An SLE, enlarged in the bottom inset, comprising an initial burst and subsequent repetitive bursts.

3.3. Drugs reported with seizure-inducing effects induce SLEs

We examined whether SLEs are commonly induced using drugs clinically reported to induce seizures in humans. We selected a total of 13 pharmacologically different drugs, including aspirin (cyclooxygenase inhibitor), cimetidine (histamine H_2 antagonist), dextran (polysaccharide), diphenhydramine (histamine H_1 antagonist), diazepam ($GABA_A$ receptor enhancer), enoxacin (DNA gyrase inhibitor), ibuprofen (cyclooxygenase2 inhibitor), imipramine (putatively noradrenaline/serotonin uptake inhibitor), ketamine (*N*-methyl-D-aspartic acid receptor inhibitor), methamphetamine (putatively catecholamine releaser and monoamine oxidase inhibitor), oseltamivir (virus neuraminidase inhibitor), strychnine (glycine receptor antagonist), and theophylline (possible adenosine receptor antagonist). The levels of these drugs in the blood in clinical use are approximately 100 μM (19), 3 μM (20), 0.01 μM (21), 0.3 μM (22), 3 μM (23), 3 μM (24), 10 μM (25), 0.3 μM (26), 3 μM (27), 3 μM (28), 3 μM (29), 1 μM (30) and 100 μM (31), respectively. For each drug, we tested 5 different concentrations. Specifically, the drugs were serially bath-applied at concentrations of 0.3×, 1×, 3×, 10×, and 30× relative to the clinical blood level for 10 min each (Table 1). Among these drugs, diphenhydramine, enoxacin, strychnine, and theophylline have been reported to frequently induce seizures in humans (32–35).

According to the representative raw LFP trace for each drug shown in Fig. 3, diphenhydramine, enoxacin, strychnine, and theophylline elicited SLEs at high concentrations, whereas the other drugs did not. Notably, psychiatric drugs, such as ketamine and methamphetamine, did not show SLEs. For each drug, we tested five brain slices, obtaining similar results, except for the two slices treated with oseltamivir or methamphetamine, in which spontaneous activity with single large potentials occurred, but it did not involve oscillatory discharges and thus was not SLEs (one case of oseltamivir is shown in Fig. 3). Therefore, we concluded that, at least in the drugs tested, this experimental system could specifically determine drugs that induce seizures in humans.

3.4. Machine learning classifications of SLEs

We next sought to develop simple statistics that automatically identify seizure-inducing drugs. To this end, we used the following two-step strategy: 1) the rough estimation of SLE candidate activity in LFP traces and 2) machine learning-based selection of true SLEs from these candidates.

We first detected large potentials whose mean slopes within a window of 1 ms were larger than 0.1 μV/ms and selected these conditions as SLE candidates. The data obtained using this simple thresholding is typically subject to false-positive detection. Basically, human eyes can easily discriminate true SLEs from erroneously detected LFP events, suggesting that deep learning, a form of the recently advanced machine learning techniques widely used to classify visual images, can precisely identify SLEs because it was originally designed as a model of the primary visual cortex (36, 37).

We first converted LFP traces into digital images in terms of time and voltage. Specifically, the LFP trace was segmented between −200 and 2070 ms relative to the initial peak of a SLE candidate and was transformed into a 227 × 227 pixel picture for which the vertical axis showed the voltage amplitude ranging from −50 to +177 μV. Thus, one pixel in the image corresponded to a square of 10 ms × 1 μV.

For the concentration of each drug, all the detected events were transformed into two-dimensional pictures that were subsequently superimposed as a single 227 × 227 picture file (Fig. 4). Consequently, we obtained 70 (=5 × 14) image files from five concentrations of 14 drugs, including picrotoxin. In these experiments, five drugs, diphenhydramine, enoxacin, picrotoxin, strychnine, and theophylline, induced SLEs, and we obtained 12 images containing SLEs with red-colored edges in Fig. 4. Again, we observed that spontaneous LFP events were also induced by other drugs, such as methamphetamine and oseltamivir, but these events were not SLEs because they contained no recurrent discharges.

We next examined whether deep learning can identify genuine SLEs (true positive detection) and reject SLE-like fake activity (true negative detection). To process the pictures, we used Caffe, the

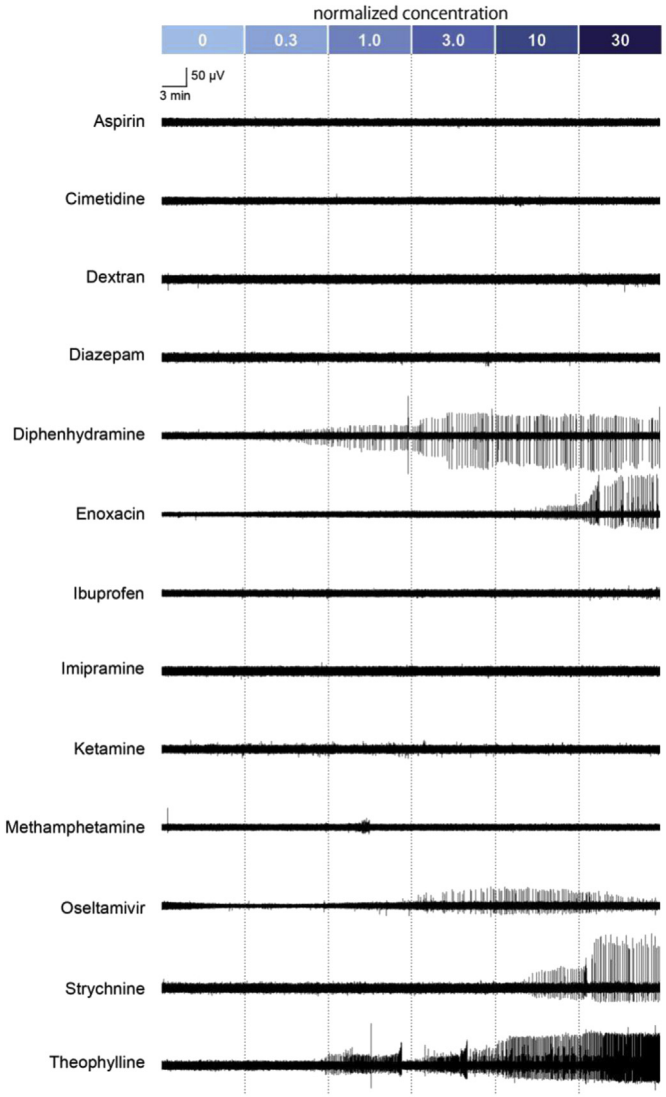

Fig. 3. Example traces of alveus LFPs recorded in the presence of 13 different drugs. The actual drug concentrations, as shown in Table 1, were normalized relative to the mean plasma concentrations reported in clinical tests in healthy persons. LFPs were recorded for 10 min at each concentration. The drugs reported to exhibit seizure-inducing AEs, including diphenhydramine, enoxacin, strychnine, and theophylline, indeed induced SLEs.

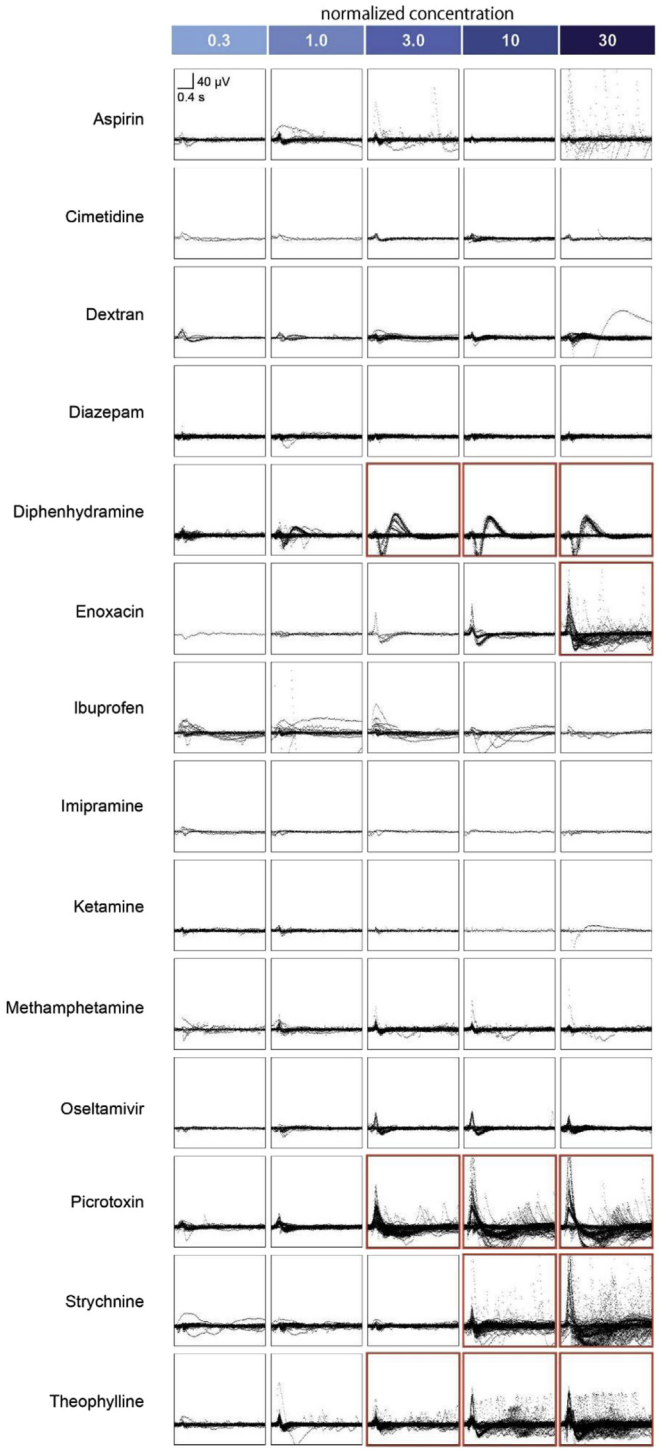

Fig. 4. LFP images. Large activity events detected from the LFP trace at each drug concentration were aligned to their onsets and superimposed onto a 227 × 227 pixel picture ($n = 5$ slices for each drug). Pictures containing at least one SLE are outlined in red.

most widely adopted open source framework for deep learning (12). Caffe extracts the semantic features of arbitrary images and expresses these features as a 4096-dimensional space in the sixth layer. Using Caffe, we converted all 70 LFP image files into 4096-dimensional vectors (Fig. 5). We subsequently applied PCA, a dimension reduction technique, to these vectors and plotted their concentration–response curves in the space of the first and second PCs, so that each data point represents a single LFP picture (*i.e.*, dose; Fig. 6A). In the PC space, the data points containing SLEs, indicated as red circles, are perfectly separated from points without SLEs by a single straight boundary defined by SVM, a supervised classifier in machine learning. Thus, all SLE-inducing drugs had at least one data point (or dose) located on the right area of the SVM-defined oblique line, whereas all data points of the other drugs were located in the left area. These results indicate that this deep learning algorithm succeeded in identifying the SLE-inducing effects of drugs.

We examined whether deep learning can 'predict' the SLE-inducing effect of a given drug based on the effects of the other drugs. We used leave-one-out cross-validation with SVM. For all 14 individual drugs, we accurately determined whether the drug was SLE-inducing based on the Caffe/PCA-determined values of the 13 remaining drugs; that is, the correct rate of the prediction was 100% (Fig. 6B).

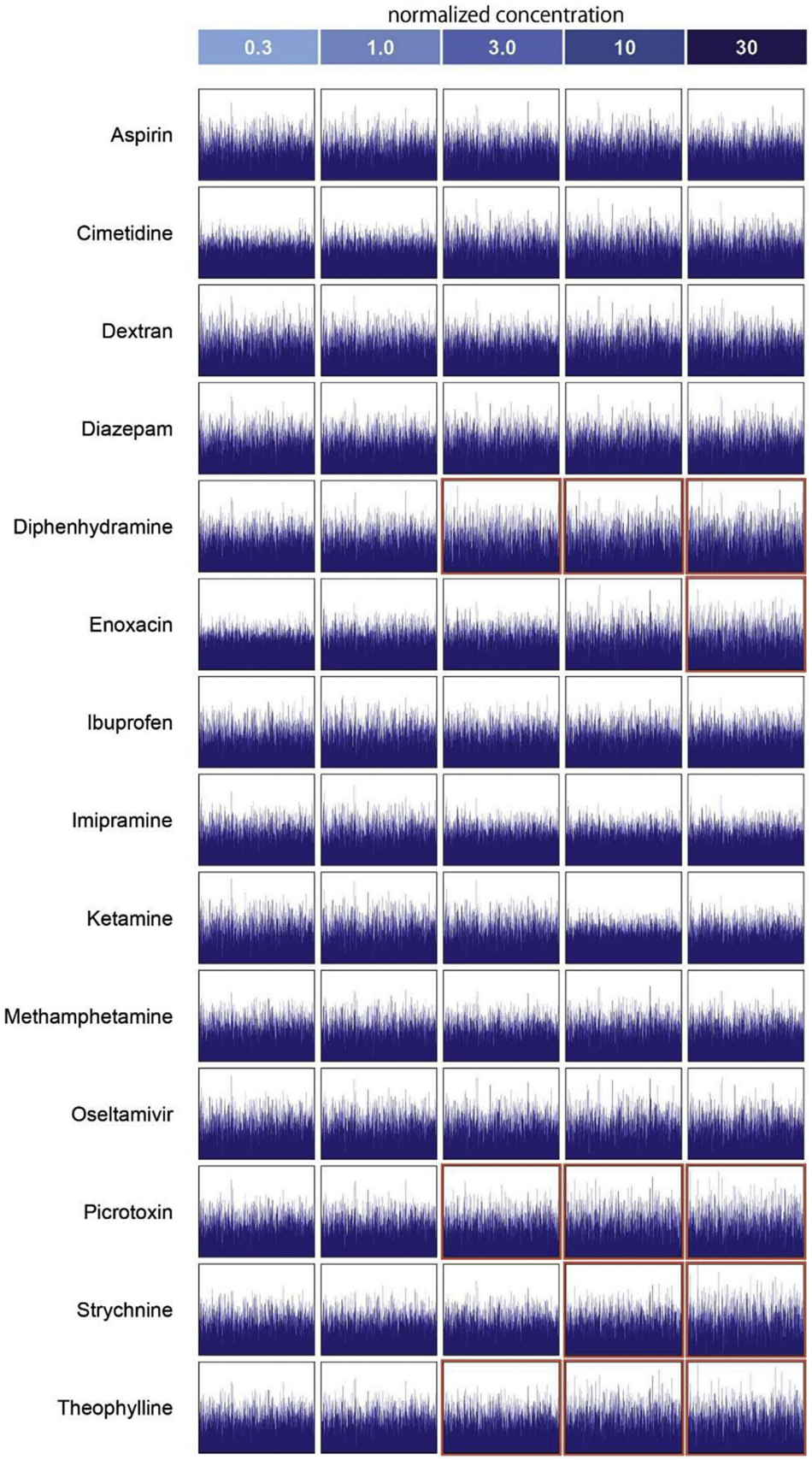

Fig. 5. Caffe-converted feature functions for LFP images. The pictures shown in Fig. 4 were processed using Caffe, and 4096 dimensional feature vectors, represented in the sixth layer of Caffe, were extracted. Each vector is shown as a histogram, with the horizontal axis showing the number of dimension (from left to right, the first to the 4096th dimension), and the vertical axis showing values at each dimension, ranging from 0 to 3. Although the horizontal axes are extremely compressed due to the graphical limitation, this figure indicates that different datasets exhibited different values in the vectors, reflecting the features in the corresponding datasets. Datasets containing SLEs are outlined in red (as in Fig. 4).

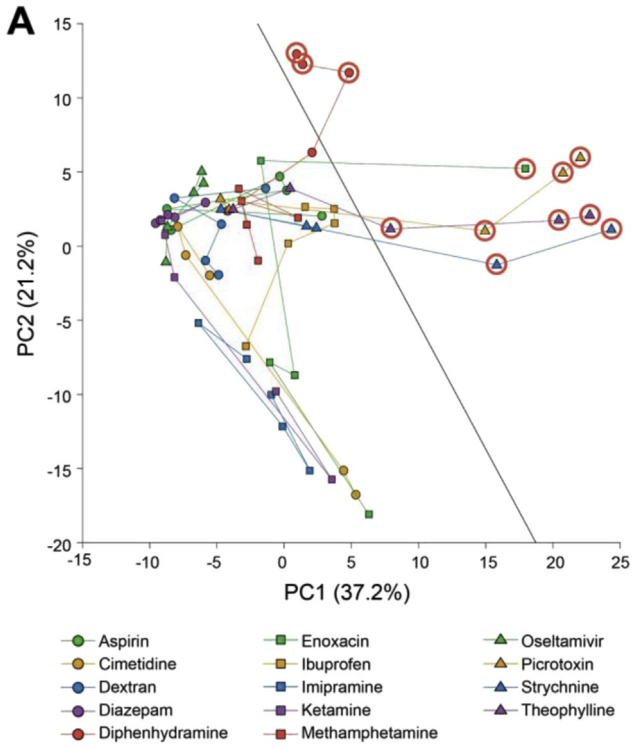

B

actual / predicted	seizure	no seizure
seizure	True Positive = 5	False Positive = 0
no seizure	False Negative = 0	True Negative = 9

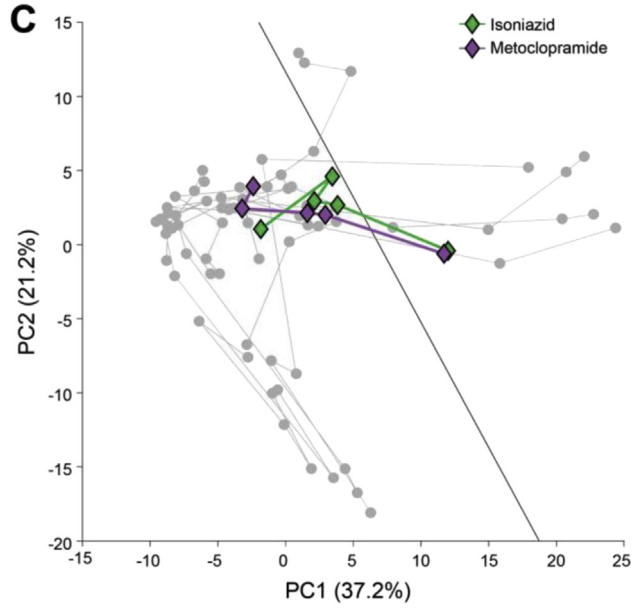

Finally, we further confirmed the validity of our prediction method, by additionally examining the effects of two completely novel, pharmacologically unrelated drugs, isoniazid (mycolic acid synthesis inhibitor) and metoclopramide (dopamine D2 antagonist), both of which have been reported to induce seizures in humans (38). The levels of isoniazid and metoclopramide in blood for clinical use are 30 μM (39) and 0.3 μM (40), respectively. We conducted the LFP recordings for isoniazid and metoclopramide and applied Caffe and PCA. Then, the feature data were superimposed onto the PC plot determined by the 14 previously tested drugs. Both drugs contained data points that were located in the right area of the boundary (Fig. 6C). Thus, we successfully predicted that isoniazid and metoclopramide are seizure-inducing.

4. Discussion

We developed a new *in vitro* system to predict the seizure-inducing effects of drugs, using LFP recordings and machine learning. We successfully used machine learning to identify the seizure-inducing drugs, diphenhydramine, enoxacin, picrotoxin, strychnine and theophylline, among a total of 14 drugs tested. Compared with manufacture data handling, this algorithm shows advantages in the speed of data processing, the long-term consistency in classification, and the detection of the potential AEs of unknown compounds.

Machine learning has recently been used to detect the onset and termination of seizure activities in EEG (41) and evaluate the seizure liability of drugs based on prediction models (42). These studies used machine learning as a simple classifier of the focused entity; thus, the present study is the first to detect epileptiform activity using machine learning through the analysis of the image data of LFP traces. In general, the dimensions of an image are substantially high and frequently mathematically intractable; notably, even the small images generated in the present study are functions with 51,229 dimensions (=227 × 227 pixels). Moreover, these images contain different levels of visual information and are not easily processed using conventional statistics or dimension reduction. To overcome this problem, we used Caffe (12). Caffe is a deep network model pre-trained to 1.2 million training images, *i.e.*, approximately 1200 images in each of 1000 categories in ImageNet (http://image-net.org/) and is thereby specialized to process visual pictures. In addition, Caffe is computationally efficient and can process one picture within 3 ms using a single commercially available graphics processing unit. Using Caffe, we extracted the visual features in LFP pictures and archived the accuracy of prediction (~100%), which is much higher than that of previously reported detectors (41, 42).

In the present study, we recorded LFPs while treating hippocampal slices with drugs in a series of concentrations under low $[Mg^{2+}]_e$ conditions. The bath application of five drugs known to have seizure-inducing effects indeed induced recurrent SLEs in this

Fig. 6. Detection and prediction of SLEs using PCA and SVM. A: Concentration-response curves in the PC space. The 4096-dimensional feature vectors were reduced in dimension using PCA and plotted in the space of the first two PCs, in which each concentration of each drug is indicated in a single point, and different concentrations of the same drug are connected with a line. Red circles indicate doses that induced SLEs (the same as Figs. 4 and 5). A boundary (black line) was defined using SVM. All data points containing SLEs were located in the right area, indicating a perfect separation of SLEs in the PC space. B: For every drug tested, the SLE-inducing effects were predicted using the leave-one-out cross-validation procedure based on SVM. The predictions were all consistent with the actual effects (*i.e.*, F1 score = 1.0; Sensitivity = 1.0; Specificity = 1.0). C: The boundary determined in Fig. 6A correctly predicted the SLE-inducing effects of two new drugs, isoniazid and metoclopramide. In both drugs, parts of data of contained points that were located in the right area of the boundary, indicating their SLE-inducing effects.

in vitro system. Diphenhydramine, a histamine H_1 receptor antagonist, which causes seizures reflecting a Na^+ channel blockade (43), actually induced SLEs. In contrast, the histamine H_2 receptor blocker cimetidine did not induce SLEs, consistent with previous reports indicating that histamine H_2 receptor antagonists do not lower the threshold for seizures (44). Enoxacin, picrotoxin, and theophylline also caused SLEs, consistent with human studies showing reliable seizure-inducing effects. One exception may be imipramine, as this drug is reported to occasionally induce seizures at a rate of 0.3–0.6% at clinical doses (45). However, we did not observe SLEs during the imipramine treatment. This discrepancy may reflect two factors: i) the number of slices tested was not sufficient, or ii) imipramine might induce SLEs at a higher concentration *in vitro*. Additional studies are necessary to increase the number of slices and concentrations. For oseltamivir, one of the five slices showed spontaneous activity events but not SLEs, likely indicating the neuropsychiatric influences of this drug, as previously reported in humans (46). To strictly investigate this neuropsychiatric effect, the use of oseltamivir carboxylate, its active metabolite, may be required.

We detected activity events from the LFP traces and superimposed these results onto a picture at each concentration for each drug. The picture was converted into a feature vector using Caffe and treated with PCA. We subsequently used SVM and successfully separated the data points representing pictures with SLEs from the other points. The PCA-based dimension reduction was likely an indispensable procedure (47) because in preliminary trials, Caffe-generated raw vectors that were not perfectly separated by SVM. This fact indicates that adopting the first two PCs reduces noise information that was not directly associated with SLEs.

The distribution of the data points of diphenhydramine in the PC space exhibited a different pattern from those of the other four seizure-inducing drugs. This fact indicates that Caffe successfully detected the differences in the original LFP images. Indeed, diphenhydramine-induced SLEs consisted of a combination of downward sinks and upward sources in LFPs, in contrast to those induced by the other four drugs, which mainly elicited upward LFP sources during SLEs. The differences in the SLE waveforms may reflect different pharmacological actions. If this is the case, our PC plot may also be applicable to analytically identify the pharmacological mechanisms underlying SLE-inducing actions.

In the detection system developed in the present study, the drugs are classified as SE-inducing or not; however, we do not currently know whether this all-or-none classification is the best strategy to predict potential AEs. Because the risks for AEs differ in degrees between drugs, further studies are needed to examine how analog ranking captures the AE risk better than all-or-none separations. Nonetheless, we propose that the approach developed herein opens an avenue for the development of a novel method for screening seizure-inducing AEs at the preclinical stage of drug development and identification of an alternative method for *in vivo* animal testing. Moreover, although we only analyzed LFP traces, the idea of deep learning-based image analysis will be applicable for electroencephalogram and calcium imaging for AE prediction.

Conflict of interest

None declared.

Acknowledgments

The authors would like to thank Dr. Takashi Shinozaki (National Institute of Information and Communications Technology) for technical support in using Caffe. This work was financially supported by the Health and Labour Sciences Research Grants for Research on Regulatory Science of Pharmaceuticals and Medical Devices from AMED No. 16mk0104006h0303 (INCENS: iPS-non clinical experiments for nervous system).

References

(1) Parent JM, Lowenstein DH. Mossy fiber reorganization in the epileptic hippocampus. Curr Opin Neurol. 1997;10:103–109.
(2) Anderson WW, Lewis DV, Swartzwelder HS, Wilson WA. Magnesium-free medium activates seizure-like events in the rat hippocampal slice. Brain Res. 1986;398:215–219.
(3) Meldrum BS. Excitatory amino acid receptors and their role in epilepsy and cerebral ischemia. Ann N Y Acad Sci. 1995;757:492–505.
(4) Sperk G, Furtinger S, Schwarzer C, Pirker S. GABA and its receptors in epilepsy. Adv Exp Med Biol. 2004;548:92–103.
(5) Nagayama T. Adverse drug reactions for medicine newly approved in Japan from 1999 to 2013: syncope/loss of consciousness and seizures/convulsions. Regul Toxicol Pharmacol. 2015;72:572–577.
(6) Lowenstein DH, Alldredge BK. Status epilepticus at an urban public hospital in the 1980s. Neurology. 1993;43:483–488.
(7) Easter A, Sharp TH, Valentin JP, Pollard CE. Pharmacological validation of a semi-automated in vitro hippocampal brain slice assay for assessment of seizure liability. J Pharmacol Toxicol Methods. 2007;56:223–233.
(8) Wong RK, Prince DA. Dendritic mechanisms underlying penicillin-induced epileptiform activity. Science. 1979;204:1228–1231.
(9) Stasheff SF, Bragdon AC, Wilson WA. Induction of epileptiform activity in hippocampal slices by trains of electrical stimuli. Brain Res. 1985;344:296–302.
(10) Mody I, Lambert JD, Heinemann U. Low extracellular magnesium induces epileptiform activity and spreading depression in rat hippocampal slices. J Neurophysiol. 1987;57:869–888.
(11) Okada M, Ishikawa T, Ikegaya Y. A computationally efficient filter for reducing shot noise in low S/N data. PLoS One. 2016;11:e0157595.
(12) Jia Y, Shelhamer E, Donahue J, Karayev S, Long J, Girshick R, et al. Caffe: convolutional architecture for fast feature embedding. arXiv. 2014;140:5093.
(13) Sasaki T, Matsuki N, Ikegaya Y. Metastability of active CA3 networks. J Neurosci. 2007;27:517–528.
(14) Sasaki T, Takahashi N, Matsuki N, Ikegaya Y. Fast and accurate detection of action potentials from somatic calcium fluctuations. J Neurophysiol. 2008;100:1668–1676.
(15) Igata H, Sasaki T, Ikegaya Y. Early failures benefit subsequent task performance. Sci Rep. 2016;6:21293.
(16) Ribak CE, Harris AB, Vaughn JE, Roberts E. Inhibitory, GABAergic nerve terminals decrease at sites of focal epilepsy. Science. 1979;205:211–214.
(17) de Curtis M, Avoli M. GABAergic networks jump-start focal seizures. Epilepsia. 2016;57:679–687.
(18) Nyikos L, Lasztoczi B, Antal K, Kovacs R, Kardos J. Desynchronisation of spontaneously recurrent experimental seizures proceeds with a single rhythm. Neuroscience. 2003;121:705–717.
(19) Bogentoft C, Carlsson I, Ekenved G, Magnusson A. Influence of food on the absorption of acetylsalicylic acid from enteric-coated dosage forms. Eur J Clin Pharmacol. 1978;14:351–355.
(20) Somogyi A, Gugler R. Cimetidine excretion into breast milk. Br J Clin Pharmacol. 1979;7:627–629.
(21) Oda H, Fukushi A, Ando E, H. T, Saito M. Relationship between intravenous small dextran and blood coagulation/fibrinolysis. Shinyaku to Rinsho. 1978;27:1853–1857.
(22) Bowden CL, Fisher JG. Relationship of diazepam serum level to antianxiety effects. J Clin Psychopharmacol. 1982;2:110–114.
(23) Paton DM, Webster DR. Clinical pharmacokinetics of H1-receptor antagonists (the antihistamines). Clin Pharmacokinet. 1985;10:477–497.
(24) Chang T, Black A, Dunky A, Wolf R, Sedman A, Latts J, et al. Pharmacokinetics of intravenous and oral enoxacin in healthy volunteers. J Antimicrob Chemother. 1988;21(Suppl. B):49–56.
(25) Mills RF, Adams SS, Cliffe EE, Dickinson W, Nicholson JS. The metabolism of ibuprofen. Xenobiotica. 1973;3:589–598.
(26) Nagy A, Johansson R. Plasma levels of imipramine and desipramine in man after different routes of administration. Naunyn Schmiedebergs Arch Pharmacol. 1975;290:145–160.
(27) Nimmo WS, Clements JA. Ketamine on demand for postoperative analgesia. Anaesthesia. 1981;36:826.
(28) Melega WP, Cho AK, Harvey D, Lacan G. Methamphetamine blood concentrations in human abusers: application to pharmacokinetic modeling. Synapse. 2007;61:216–220.
(29) Ariano RE, Sitar DS, Zelenitsky SA, Zarychanski R, Pisipati A, Ahern S, et al. Enteric absorption and pharmacokinetics of oseltamivir in critically ill patients with pandemic (H1N1) influenza. CMAJ. 2010;182:357–363.
(30) Perper JA. Fatal strychnine poisoning–a case report and review of the literature. J Forensic Sci. 1985;30:1248–1255.
(31) Morishita N, Tomono Y, Hasegawa J, Nemoto T, Kuwabara H, Tsuchiya S, et al. Bioequivalence and pharmacokinetics of a new theophylline slow release formulation, E-0686. Jpn Soc Clin Pharmacol Ther. 1985;16:705–718.

(32) Thundiyil JG, Kearney TE, Olson KR. Evolving epidemiology of drug-induced seizures reported to a poison control center system. J Med Toxicol. 2007;3:15–19.
(33) Simpson KJ, Brodie MJ. Convulsions related to enoxacin. Lancet. 1985;2:161.
(34) Cooling DS. Theophylline toxicity. J Emerg Med. 1993;11:415–425.
(35) Makarovsky I, Markel G, Hoffman A, Schein O, Brosh-Nissimov T, Tashma Z, et al. Strychnine–a killer from the past. Isr Med Assoc J. 2008;10:142–145.
(36) Wan J, Wang D, Hoi SCH, Wu P, Zhu J, Zhang Y, et al. Deep learning for content-based image retrieval: a comprehensive study. Proc ACM Int Conf Multimed. 2014;22:157–166.
(37) LeCun Y, Bengio Y, Hinton G. Deep learning. Nature. 2015;521:436–444.
(38) Romero JA, Kuczler Jr FJ. Isoniazid overdose: recognition and management. Am Fam Physician. 1998;57:749–752.
(39) Boxenbaum HG, Berkersky I, Mattaliano V, Kaplan SA. Plasma and salivary concentrations of isoniazid in man: preliminary findings in two slow acetylator subjects. J Pharmacokinet Biopharm. 1975;3:443–456.
(40) Ross-Lee LM, Eadie MJ, Hooper WD, Bochner F. Single-dose pharmacokinetics of metoclopramide. Eur J Clin Pharmacol. 1981;20:465–471.
(41) Shoeb A, Kharbouch A, Soegaard J, Schachter S, Guttag J. A machine-learning algorithm for detecting seizure termination in scalp EEG. Epilepsy Behav. 2011;22(Suppl. 1):S36–S43.
(42) Zhang H, Li W, Xie Y, Wang WJ, Li LL, Yang SY. Rapid and accurate assessment of seizure liability of drugs by using an optimal support vector machine method. Toxicol In Vitro. 2011;25:1848–1854.
(43) Jang DH, Manini AF, Trueger NS, Duque D, Nestor NB, Nelson LS, et al. Status epilepticus and wide-complex tachycardia secondary to diphenhydramine overdose. Clin Toxicol (Phila). 2010;48:945–948.
(44) Scherkl R, Hashem A, Frey HH. Histamine in brain–its role in regulation of seizure susceptibility. Epilepsy Res. 1991;10:111–118.
(45) Rosenstein DL, Nelson JC, Jacobs SC. Seizures associated with antidepressants: a review. J Clin Psychiatry. 1993;54:289–299.
(46) Toovey S, Rayner C, Prinssen E, Chu T, Donner B, Thakrar B, et al. Assessment of neuropsychiatric adverse events in influenza patients treated with oseltamivir: a comprehensive review. Drug Saf. 2008;31:1097–1114.
(47) Gong Y, Wang L, Guo R, Lazebnik S. Multi-scale orderless pooling of deep convolutional activation features. arXiv. 2014;1403:1840.